

See discussions, stats, and author profiles for this publication at: <https://www.researchgate.net/publication/273775861>

The Performance of Solar Air Heater with High Density Polyethylene Paper as Top Cover and Brown Sand Layer as an Absorber

Article · June 2014

DOI: 10.14355/ijes.2014.0403.03

CITATIONS

0

READS

96

4 authors, including:



Francis Ndiritu

Egerton University

26 PUBLICATIONS 47 CITATIONS

[SEE PROFILE](#)



Paul Kamweru

Leibniz Institute on Aging – Fritz Lipmann Institute

23 PUBLICATIONS 28 CITATIONS

[SEE PROFILE](#)

Some of the authors of this publication are also working on these related projects:



Ultraviolet-Irradiated Mushrooms [View project](#)



Kinetochores Structure Elucidation [View project](#)

The Performance of Solar Air Heater with High Density Polyethylene Paper as Top Cover and Brown Sand Layer as an Absorber

Njoroge G. Ndegwa^{*1a}, Ndiritu F.G.^{2a}, Golicha Hussein^{3a} Kamweru P. K. ^{4b}

^a Egerton University, Physics Department, P.O.Box 536 Egerton-20115, Kenya

^b Chuka University, Department of physical sciences, P.O.Box 107 Chuka-60400, Kenya

^{*1}georgend02@gmail.com; ²fgichukin@yahoo.com; ³golicha2000@yahoo.com; ⁴pkkamweru@chuka.ac.ke

* Corresponding author

Received 7 November 2012; Revised 18 February 2014; Accepted 18 February 2014; Published 16 April 2014
© 2014 Science and Engineering Publishing Company

Abstract

Experimental investigations on the performance of a flat plate solar air heater (SAH) with brown sand as absorber and clear HDPE paper as top cover was done. The efficiency, heat gain factor and heat loss coefficient were determined for the collector. The effects of air mass flow rate and thermal efficiency was also studied. The SAH model was placed outdoors and tests were conducted in an open field between 0900 and 1500 Hrs. and parameters including solar radiation, temperature and air mass flow rates were recorded after every 20 minutes for 100 hours. Results show that, the efficiency increase with increasing air mass flow rate. The highest efficiency obtained was 54% at air mass flow rate of 1.22×10^{-5} Kg/s. The temperature difference between the outlet flow and the ambient reduces as the air mass flow rate increases with a maximum difference of 31°C at air mass flow rate of 6.83×10^{-6} Kg/s which occurred at 1240 Hrs.

Keywords

Solar Air Heaters; Heat Removal Factor; Collector Overall Heat Loss Coefficient; Thermal Performance

Introduction

SAHs are used in space heating, drying and paint spraying operations. Numerous SAH devices have been developed and used experimentally (Ho et al. 2005). A glass or plastic cover is fixed above the absorber plate and the system is insulated thermally from the back and the sides. SAHs are simple in design and maintenance. Corrosion and leakage problems are less severe compared with liquid heater solar systems (Ozgen et al. 2009). The main drawback of a SAH is that the heat-transfer coefficient between

the absorber plate and the air stream is low, which results in a lower thermal efficiency of the heater (Ozgen et al. 2009). However, different modifications are suggested and applied to improve the heat-transfer coefficient between the absorber plate and air (Ozgen et al. 2009). There are various factors affecting the SAH efficiency. These include collector length, collector depth, type of absorber plate, glass cover plate, wind speed, etc. Increasing the absorber plate shape area will increase the heat-transfer to the flowing air, but on the other hand, will increase the pressure drop in the collector; this increases the required power to pump the air flow crossing the collector (Esen, 2008). Performance improvement can be achieved using diverse materials, various shapes and different dimensions and layouts. The modifications to improve the heat-transfer coefficient between the absorber plate and air include the use of an absorber with fins attached, corrugated absorber, matrix type absorber, with packed bed, with baffles and different configurations are given in the literature (Yeh et al. 2000, Yeh et al. 2002, Esen 2008, Ozgen et al. 2009)

Several configurations and designs, with different shapes and dimensions of the air flow passage in plate type solar air collectors have been tested (Hollands and Shewan 1981; Choudhury and Garg 1991; Hachemi 1995; Yeh et al. 1999; Hegazy 2000; Yeh et al. 2000). The double-flow type SAHs have been introduced for increasing the heat-transfer area, leading to improved thermal performance (Yeh et al. 1999; Yeh et al. 2002). The increases of thermal energy

between the absorber plate and the air, which clearly improves the thermal performances of the solar collectors with obstacles arranged into the air channel duct. These obstacles allow a good distribution of the fluid flow (Esen 2008; Zaid et al. 1999; Moumami et al. 2004). Sahu and Bhagoria (2005) planned to investigate the effect for different pitch of 90° broken wire rib roughness on the enhancement of thermal performance of SAH. Ghoneim (2005) investigated the effects of gap thickness on the performance of compound honeycomb using the solar collector. Sadasuke et al. (2008) investigated the performance of a collector with a flow in the upper channel on the absorber plate as well as in the lower channel. Njomo (2000) examined the unsteady state heat exchanges governing the functioning of an unglazed one-pass SAH utilizing a non-porous selective absorber. The mathematical model developed is then used to predict the thermal performances of such a collector. Karim and Hawlader (2006) investigated both experimentally and theoretically in an effort to improve the performance of conventional air heaters using finned and v-corrugated air heaters. Esen (2008) compared between the results obtained in the case of the double-flow SAH supplied with obstacles and those of the collector without obstacles. The influences of various parameters, such as the obstacles of absorber plate, the mass flow rate of air and the level of absorber plates in duct, on the energetic efficiencies of the SAH were examined and the significant variables were identified. This paper presents an analysis of efficiency evaluation of a new single-pass SAH. Two different absorbing plates have been tested in this study. An experimental set-up was designed, constructed and tested outside the Physics LAB 2 in the Faculty of Science, Egerton University, Njoro - Kenya. The efficiency of the new SAH was determined from the experimental measurements.

Experimental Set-up and Measurement Procedure

An experimental SAH model was constructed and tested outside the Physics LAB 2 of Egerton University, Njoro. The university is located in Njoro District in the greater Nakuru County on the eastern edge of the Mau Forest Complex, the largest single forest block in Kenya. The area lies between the forest and Lake Nakuru National Park, a world famous flamingo habitat. The greater Nakuru County is situated between 35° 28' - 35° 36' E longitude and 0° 13' - 1° 10' S latitude. Njoro stands at an altitude of 1,800 m (6,000

ft) above sea level and has a mild, agreeable climate. Temperatures range between 17-22° C, while the average annual rainfall is in the region of 1,000 mm (Walubengo, 2007). A schematic view of experimental setup of the constructed SAH system is shown in Figure 1.

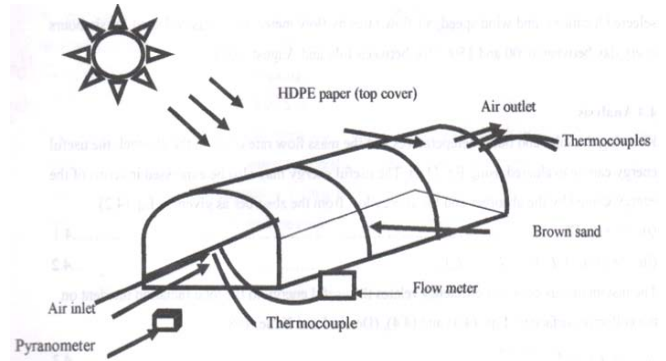


FIGURE 1 EXPERIMENTAL PROTOTYPE MODEL OF A SAH

In this study, two types of absorber plates (Brown and Grey sand) were investigated. Brown sand was used due to its high Absorptance value of 59% as compared to grey sand whose Absorptance value was found to be 56%, this is due to the difference in their colors. Different types of top cover materials were also investigated in order to determine the best. Clear HDPE paper was found to have the highest Transmittance value of 84% as compared to LDPE and Glass whose Transmittance values were found to be 72% for each. The absorber surface is the most important component of the collector since absorbs the sun's radiation. Thermal losses through the backs of the collector are mainly due to the conduction across the insulation (thickness 3 cm) and those caused by the wind and the thermal radiation of the insulation is assumed negligible. Thermocouples were positioned evenly on the top surface of the absorber plate, at identical positions along the direction of flow, where Inlet, outlet and ambient air temperatures were measured by well-insulated thermocouples. The total solar radiation incident on the surface of the collector was measured with a Kipp and Zonen CM 3 Pyranometer. This meter was placed adjacent to the glazing cover, at the same plane. The total solar radiation was recorded manually. The variables were recorded at time intervals of 20 minutes and include: insolation, inlet and outlet temperatures of the working fluid circulating through the collectors, ambient temperature, absorber plate temperatures at several selected locations, wind speed and air flow rates. Data was collected for six hours in non-cloudy days between 0900 and 1500 Hrs. between July and

August, 2011. The speed and direction of wind was assumed to be constant.

Analysis

Knowing the inlet and outlet temperatures and the mass flow rate of air in the channel, the useful energy can be evaluated using Eq. (4.1). The useful energy may also be expressed in terms of the energy gained by the absorber and the energy lost from the absorber as given by

$$Q_{ux} = C_p(T_i - T_a) \tag{1}$$

$$Q_{ux} = F_R(\tau\alpha)A_cI - F_RU_LA_c(T_i - T_a) \tag{2}$$

The instantaneous collector efficiency relates the useful energy to the total radiation incident on the collector surface by Eqs. (3) and (4), (Demirel and Kunc, 1987).

$$\eta = \frac{Q_u}{A_cI} = \frac{C_p(T_i - T_a)}{A_cI} \tag{3}$$

$$\eta = \frac{Q_u}{A_cI} = F_R(\tau\alpha) - F_RU_L \frac{(T_i - T_a)}{I} \tag{4}$$

The collector performance is determined by three parameters F_R , U_L and $(\tau\alpha)$. These parameters depend on construction materials, flow conditions and design type of the collector. The collector heat removal factor, F_R , is the heat-transfer capacity of collector. It is a measure of the heat transferred to the fluid flowing through the absorber. U_L is the global heat loss coefficient. The term $(\tau\alpha)$, represents the optical properties of the system; τ is the transmittivity of transparent cover and α is the absorptivity of the absorber surface.

Eq. 4 indicates that a plot of instantaneous efficiency values against $\frac{(T_i - T_a)}{I}$ will result to a straight line whose slope and intercept are F_RU_L and $F_R(\tau\alpha)$, respectively. For $\eta = 0$, $\Delta T = T_p - T_a$. Thus, if the optical properties of the system are known F_R and U_L can be determined.

Results and Discussions

Typical values of solar radiation and ambient temperatures between 0900 and 1500 Hrs. are shown in Figures 2 and 3. Solar radiation is at their highest values at about 1300Hrs. as is expected. The solar radiation decreases as the time passes through 1300 Hrs.

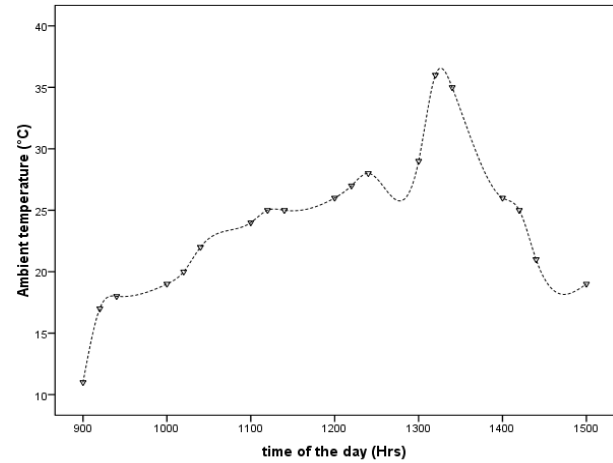


FIGURE 2 AVERAGE VALUES OF SOLAR TEMPERATURES WITH TIME

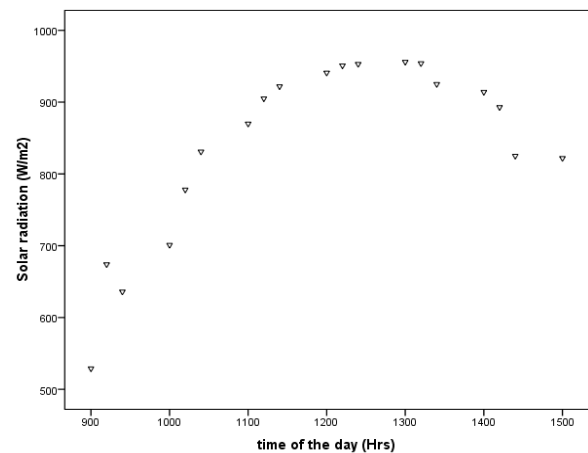


FIGURE 3 AVERAGE VALUES OF SOLAR RADIATION WITH TIME

The Ambient temperature also increases with time of the day until 13.00 pm and starts to decrease thereafter. The variation is not linear due to cloudy sky sometimes. Figure 4 shows the relationship between the change in temperature (difference between air inlet and outlet temperatures) and daily instantaneous solar radiation. The ambient temperature was between 10 and 40°C with the highest at 36°C. The inlet temperatures were similar to ambient temperature. The temperature differences between the inlet and outlet temperatures can be compared directly when determining the performance of the collectors. Since the amount of instantaneous radiation is the most important parameter in solar collectors, these changes are expected.

The highest daily solar radiation is obtained as 956W/m². As expected, it increases in the morning to a peak value of 956 W/m² at 1300 Hrs. and starts to decrease afterwards. The other parameters as air inlet and outlet temperatures exhibit parallel changes with the instantaneous radiation, i.e. they depend directly

on the amount of direct solar radiation for all air flow rates.

Information on the temperature rise of air with solar radiation is important when designing solar air heaters. If the inlet temperature is close to the ambient temperature, the temperature rise varies almost linearly with solar radiation. The variation of temperature difference with incident radiation for the collector, presented in Figure 4, is in an agreement with this observation. The scattering of the solar radiation due to cloudy sky conditions results in departure from the linearity in the Figures. These plots of temperature difference versus insolation may be helpful to estimate the fluid temperature for any time of the day with the help of available meteorological data (Akpinar and Kocyyigit, 2010). The maximum temperature increase (ΔT) through solar air heater is 31°C for 6.83×10^{-6} Kg/s air mass flow rate, and occurred at 1240 Hrs. It was also essential to study the variation of ΔT with air mass flow rate. The information is important in determining the optimum air mass flow rate for a greater ΔT . Figure 5 was obtained.

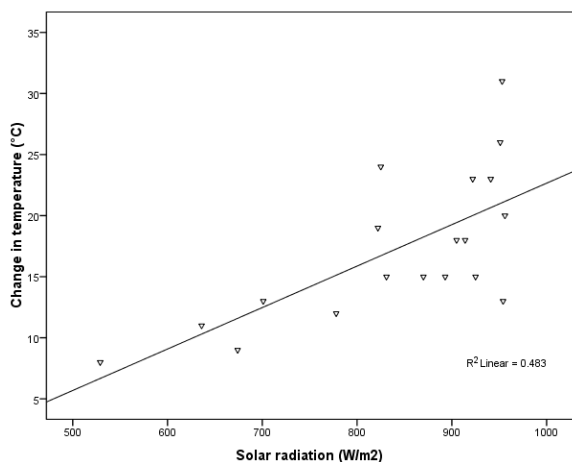


FIGURE 4 VARIATION OF TEMPERATURE DIFFERENCE AND AVERAGE INSTANTANEOUS SOLAR RADIATION

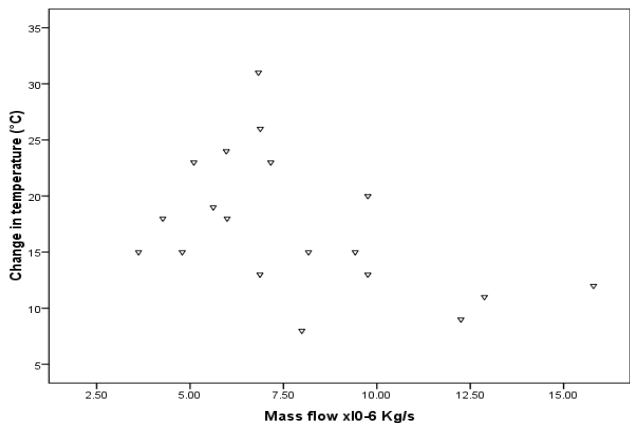


FIGURE 5 VARIATION OF TEMPERATURE DIFFERENCE AND AIR MASS FLOW RATE

Figure 6 shows that ΔT increases to a maximum of 31°C for air mass flow rate of 6.8329×10^{-6} Kg/s implying that for this air heater, this is the optimum flow rate. ΔT reduces afterwards due to the change in flow from laminar or turbulent. The variation is not linear due to natural flow of air. The values of conversion efficiency into heat energy of incident solar radiation on the collector were computed by using data from the daytime measurements between 0900Hrs and 1500Hrs. In order to determine F_R and U_L , a graph of collector efficiency versus the temperature parameter $(T_i - T_a)/I$ for the SAH at different mass flow rate was drawn as shown in Figure 7.

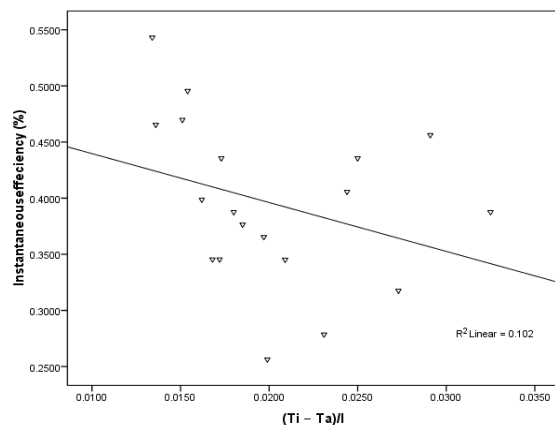


FIGURE 6 VARIATION OF AVERAGE INSTANTANEOUS EFFICIENCY AND $(T_i - T_a)/I$

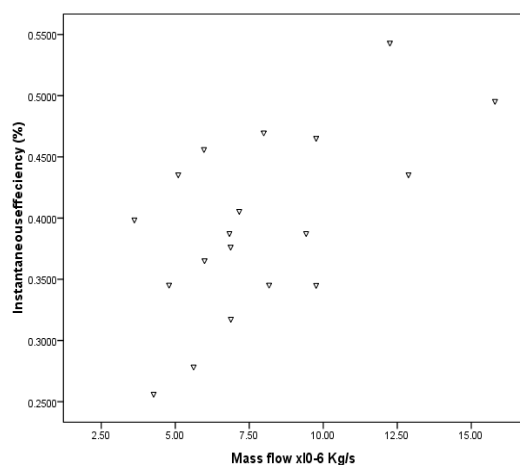


FIGURE 7 VARIATION OF AVERAGE INSTANTANEOUS EFFICIENCY AND AIR MASS FLOW RATE

The maximum efficiency for the SAH was found to be 54% and occurred at 0920 Hrs. The data in Figure 6 is fitted to straight lines using SPSS software version 16.0. The scatter of the data around the straight line is mainly attributed to the angle of incidence variations, wind speed, variations in air mass flow rates and the dependence of the heat loss on the plate temperature (Kocyyigit et al. 2009). Also, the variations of the

relative proportions of beam diffuse and ground reflective components of solar radiation are participating in the data scattering. Thus, scatters in the data are to be expected (Abdullah et al. 2003, Karsli 2007). From Figure 4.6, it is evident that the efficiency decreases as the temperature parameter increases. The higher the temperature parameter the less the efficiencies are resulted. This means, at higher temperature parameters, the overall loss is high. It was also important to determine the relationship between the efficiency and the air mass flow rate Figure 7 demonstrates this.

TABLE A2 VARIATION OF SOLAR RADIATION, TEMPERATURE CHANGE, AIR MASS FLOW RATE, QUOTIENT OF TEMPERATURE CHANGE WITH SOLAR RADIATION, EFFICIENCY AND AMBIENT TEMPERATURE

Time (Hrs)	Solar Radiation (W/m ²)	ΔT (C)	Mass flow x10 ⁻⁶ Kg/s	ΔT / I (°C m ² AV)	Efficiency	Ambient (°C)
0900	529	08	7.99	0.0151	0.4698	11.0
0920	674	09	12.25	0.0134	0.5432	17.0
0940	636	11	12.88	0.0173	0.4356	18.0
1000	701	13	6.87	0.0185	0.3765	19.0
1020	778	12	15.80	0.0154	0.4956	20.0
1040	831	15	9.42	0.0180	0.3876	22.0
1100	870	15	8.17	0.0172	0.3454	24.0
1120	905	18	4.27	0.0199	0.2564	25.0
1140	922	23	5.10	0.0250	0.4356	25.0
1200	941	23	7.16	0.0244	0.4057	26.0
1220	951	26	6.88	0.0273	0.3176	27.0
1240	953	31	6.83	0.0325	0.3876	28.0
1300	956	20	9.76	0.0209	0.3452	29.0
1320	954	13	9.76	0.0136	0.4654	36.0
1340	925	15	3.62	0.0162	0.3987	35.0
1400	914	18	5.99	0.0197	0.3654	26.0
1420	893	15	4.79	0.0168	0.3454	25.0
1440	825	24	5.97	0.0291	0.4563	21.0
1500	822	19	5.62	0.0231	0.2786	19.0
Average	841	17	7.92	0.0201	0.3953	28.8

From Figure 6, it can be seen that, the collector efficiency increases with increasing air mass flow rate of air considerably. The variation can be attributed to changes in flow condition from laminar to turbulent. From Figure 6, it can be seen that the slope of the efficiency curves decreases, meaning decrease in loss coefficient, with increase of mass flow rates. The values of F_R , and U_L were calculated from the slopes and intercepts of the best lines in Figure. 6. The values of F_R and U_L were found to be 0.84 and 7.98 W/m²K respectively. This is comparable to the data obtained by Kocuyigit et al. (2009) where they found that the heat

loss coefficients are 24.17 and 19.3 W/m²K, at $\dot{m} = 0.0074$ Kg/s and $\dot{m}=0.0052$ Kg/s respectively for a flat plate SAH with absorber plate which has been plated with cooper plate that's been painted black. This indicates that heat loss coefficient decreases with air mass flow rate. It can be seen that the heat removal factor and global heat coefficient are high for the measured air flow rates. Table A2 contains data used to draw the graphs.

Conclusions

This study shows that for a single pass solar air heater using brown sand as absorber plate and HDPE paper as top cover, there is a significant increase in the thermal efficiency of the air heater. The efficiency increases when the air mass flow increases due to an enhanced heat-transfer to the air flow. Also, the efficiency increases as the temperature parameter increases, meaning, at higher temperature parameter, the overall loss is lower. The temperature difference between the outlet flow and the ambient ΔT , reduce with an increase in the air mass flow rate. Further, results showed that the collector temperature difference increase with increasing solar radiation, I, and decreases as solar radiation drops to lower values later on during the day. The maximum temperature difference obtained from this study is 31°C. The maximum thermal efficiency obtained is 54.32% for air mass flow rate of 1.2x10⁻⁵ Kg/s.

General Recommendations

- (i) In this research, there was a limitation on measurement of IR by the Optical Spectrum Analyzer (Spectro 320) at higher wavelength range of above 880 nm due to the limitation of the analyzer. Research should be carried out to investigate the behavior of optical properties of HDPE, LDPE and brown sand at higher wavelength range (880-2450 nm).
- (ii) The flow meter used in this research measures air flow rate in m³/h which is then converted mathematically to Kg/s for use in the research. The conversion leads to errors and thus, an orifice meter or any other appropriate equipment may be used in order to reduce the error in the conversion.
- (iii) The heated air requires to be kept for use when there is no sun shine or during the night thus, there is need to research on appropriate

methods of keeping the heat produced for future use.

REFERENCES

- Choudhury C. and Garg H.P. (1991). Design analysis of corrugated and flat plate solar air heaters. *Renewable Energy*; 1: 595-607.
- Esen H. (2008). Experimental energy and energy analysis of a double-flow solar air heater having different obstacles on absorber plates. *Building Environment*; 43:1046-1054.
- Hollands K.G.T. and Shewan E.C. (1981). Optimization of flow passage geometry for air heating plate-type solar collectors. *Solar Energy*; 103:323-334.
- Hachemi A. (1995). Thermal performance enhancement of solar air heaters by fan-blown absorber plate with rectangular fins. *International Journal of Energy*; 19: 567-568
- Hegazy A. A., (2000). Performance of flat plate solar air heaters with optimum channel geometry for constant variable flow operation. *Energy Conversion Management* ; 41: 401 – 402.
- Ho CD., Yeh H.M. and Wang R.C. (2005) Heat-transfer enhancement in double-pass flat-plate solar air heaters with recycle. *Journal of Energy*; 30:2796-2817.
- Moumni N, Ali S.Y, Moumni A, Desmons J.Y. (2004). Energy analysis of a solar air collector with rows of fins. *Renewable Energy*; 29: 2053-2064.
- Njomo D.(2000). Unglazed selective absorber solar air collector: heat exchange analysis. *Heat Mass Transfer*; 36: 313-327.
- Karim M. A. and Hawlader M.N.A., (2006). Performance investigation of flat plate, v-corrugated a tinned air collectors. *Energy*; 31: 452- 470.
- Ozgen F., Esen M. and Esen H. (2009). Experimental investigation of thermal performance of a double-flow solar air heater having aluminum cans. *Renewable Energy*; 34:2391-2398.
- Sahu MM. and Bhaeoria J.L., (2005). Augmentation of heat transfer coefficient by using 90° broken transverse ribs on absorber plate of solar air heater. *Renewable Energy*; 30:2057-2073.
- Yeh H.M., Ho CD. and Hou J.Z. (2002). Collector efficiency of double-flow solar air heaters with fins attached. *Energy*; 27:715-727.
- Yeh HM, Ho C. D., Lin C. Y. (2000). Effect of collector aspect ratio on the collector efficiency of upward type baffled solar air heaters. *Energy Conversion Management*; 41:971-981.
- Yeh H.M., Ho CD. and Hou J.Z. (1999). The improvement of collector efficiency in solar air heaters by simultaneously air flow over and under the absorbing plate. *Energy*; 24: 857-871.